Appl. Num. Math. 29, 31-43, 1999

Reversible Adaptive Regularization Methods for Atomic N-body Problems in Applied Fields ⋆

Benedict Leimkuhler

Dept. of Mathematics, 405 Snow Hall, University of Kansas, Lawrence, KS 66045, USA. leimkuhl@math.ukans.edu.

Abstract

Reversible and adaptive integration methods based on Kustaanheimo-Stiefel regularization and modified Sundman transformations have recently been proposed for perturbed Kepler motion and certain types of N-body problems including atomic scattering and gravitation. These methods are explicit and demonstrate superior conservation properties compared to standard explicit integrators applied with or without variable stepsize schemes. In this note, reversible adaptive regularization is applied to treat (classical) atomic systems in applied electrical and/or magnetic fields.

Key words: adaptive methods, time-reversible variable stepsizes, Hamiltonian systems, few-body problems, scattering, N-body problems, regularization, time-transformations, perturbed Kepler motion

AMS(MOS) Subject Classifications: 65L07, 70H15

1 Introduction

Time-reversal symmetry is a strong geometric property frequently associated to physical (mechanical) Hamiltonian problems. Methods which preserve the time-reversal symmetry exhibit improved stability in long term simulations [7,10,13,18,27] compared to standard integration methods. An example of an explicit, efficient and time-reversible integration method is the Störmer-Verlet scheme, a popular integrator for chemical and physical N-body problems.

⋆ This research was supported by NSF grant DMS-9303223 and was conducted while the author was visiting Cambridge University.

In [2,13], it was shown that a general Sundman time transformation could be treated in an explicit, time-reversible way. These "Adaptive Verlet" methods can be viewed as time-reversible variable stepsize methods, and they prove to be very useful for treating problems with a wide variation in the intensity of the vector field. However, for N-body problems involving Coulomb-type singularities, even the Adaptive Verlet methods may fail or become inefficient, due to extremely strong forces present during the two-body close approach. In this case, it is necessary to perform some type of coordinate regularizations in addition to whatever time-transformations may be needed.

A method was proposed in [18] for combining Adaptive Verlet schemes with Kustaanheimo-Stiefel transformations. This approach has been found to be effective for perturbed Kepler problems and N-body problems such as the atomic system consisting of a nucleus and several surrounding electrons. The interest in atomic problems of this type is connected to semiclassical methods and is becoming a standard approach to certain types of atomic simulations. These problems frequently include applied fields of some sort (electrical, magnetic, etc.). Moreover, magnetic-field like terms occur in gravitational problems as the effective description of perturbing terms [9].

In this note, we first outline the reversible adaptive regularization (RAR) method of [18] giving a detailed description of the algorithm, then consider its generalization to problems with applied fields.

2 Background

A Hamiltonian system is said to possess time-reversal symmetry if its energy H is invariant under the mapping $R : p \to -p$,

$$H(q,p) = H(q,-p)$$

Let the flow map of the system be defined by Φ_τ, i.e.

$$\begin{bmatrix} q(\tau) \\ p(\tau) \end{bmatrix} = \Phi_\tau \left(\begin{bmatrix} q(0) \\ p(0) \end{bmatrix} \right),$$

then for a time-reversible Hamiltonian system

$$\Phi_\tau \circ R = R \circ \Phi_{-\tau}.$$

(The latter equation can be taken as a definition of time-reversibility for more general differential equation systems.)

An example of a time-reversible system is the N-body problem. We assume that the positions are $q = (q_1, q_2, \ldots, q_N)$, where each $q_i \in \mathbf{R}^3$, and let p_i represent the corresponding momenta. (We will later use superscripts to indicate the timestep index.) The Hamiltonian of the N-body problem divides into two parts:

$$H = T(p) + V(q),$$

where T is the kinetic energy

$$T(p) = \sum_{i=1}^{N} \frac{|p_i|^2}{2m_i},$$

and the potential energy $V(q)$ is assumed to decompose into Coulombic two-body interactions:

$$V(q) = \sum_{i=1}^{N-1} \sum_{j=i+1}^{N} \frac{\alpha_{ij}}{r_{ij}},$$

where $r_{ij} = |q_i - q_j|$. For gravitation, all of the coefficients α_{ij} are negative, whereas for atomic problems, both signs occur. To simplify the presentation, we will typically assume unit masses and that the constants α_{ij} are ± 1.

An important special situation in which we are interested is the mono-atomic system consisting of a single fixed nucleus (at the origin) and multiple electrons.

3 Reversible Integration with Time and Coordinate Transformations

To integrate the N-body problem, we can use the natural splitting of the Hamiltonian into kinetic and potential parts, solving first one then the other, serially. Better, we may integrate the Hamiltonian system with energy V for half a timestep, then that with energy T for a timestep, then that with energy V again for half a timestep. This yields the Störmer-Verlet method:

$$p^{n+1/2} = p^n - \frac{1}{2} h \nabla V(q^n)$$

$$q^{n+1} = q^n + hp^{n+1/2}$$
$$p^{n+1} = p^{n+1/2} - \frac{1}{2}h\nabla V(q^{n+1})$$

where h is the stepsize, and the superscripts indicate the timestep. The elegant simplicity of this strategy is complemented by its efficiency (one force evaluation per timestep), its accuracy (second order with a moderate error constant), and its stability (a large interval of stability on the imaginary axis). The method has remained a standard for N-body integration throughout the era of computers, and it continues to be a favorite in molecular dynamics.

A theoretical argument in [18] indicates how the reversible method applied properly to a two-body integration (e.g. Kepler problem), automatically preserves orbital axial symmetry. This results in improved energy conservation, even in perturbed two-body problems, and explains the observed superior performance of reversible integrators for treating N-body problems dominated by two-body collisions. Experiments conducted by the author indicate that when three-body approaches are present, the performance of reversible methods can be seriously degraded. In many cases, e.g. Coulombic N-body problems, the two-body approaches do in fact dominate and three-body collisions are extremely rare [26].

3.1 Time-Transformation

When the forces vary greatly with time, the simulation results can often be improved by incorporating a *time-transformation*. A Sundman time-transformation is a vector-field rescaling corresponding to the additional equation

$$\frac{dt}{d\tau} = g(q,p)$$

One typically assumes g is smooth and positive, and that $g(q,-p) = g(q,p)$. The differential equations in the reparameterized time variable τ become

$$\frac{d}{d\tau}q = g\nabla_p H,$$
$$\frac{d}{d\tau}p = -g\nabla_q H.$$

The new system is no longer Hamiltonian, but it can be shown to retain the time-reversal symmetry. [1] A simple approach to integrating the rescaled vector

[1] The alternative is to use a Poincaré transformation $H \to \tilde{H} = g(H - H_0)$ which has certain advantages and disadvantages, see [10,20].

field is to use the Adaptive Verlet strategy of [2,13]:

$$
\begin{aligned}
p^{n+1/2} &= p^n - \frac{1}{2} h_n \nabla V(q^n), \\
q^{n+1/2} &= q^n + \frac{1}{2} h_n p^{n+1/2}, \\
q^{n+1} &= q^{n+1/2} + \frac{1}{2} h_{n+1} p^{n+1/2}, \\
p^{n+1} &= p^{n+1/2} - \frac{1}{2} h_{n+1} \nabla V(q^{n+1}).
\end{aligned}
$$

where the stepsize is updated by one of several possible formulae, e.g.

$$
\frac{1}{h_n} + \frac{1}{h_{n+1}} = \frac{2}{g(q^{n+1/2}, p^{n+1/2}) \Delta\tau}.
$$

In this formula, $\Delta\tau$ is a fixed parameter which controls the accuracy of the simulation, much like the stepsize in a fixed stepsize simulation or the local error tolerance in a traditional variable stepsize method. The unusual form of the stepsize update is a consequence of stability considerations and will be discussed in more detail in a forthcoming article.

3.2 Coordinate Transformations

A *coordinate transformation* can also be incorporated into the reversible framework by splitting off the Keplerian part. In fact, the best approach appears to be based on a combination of coordinate and time transformation. As a simple example, we consider the Kepler problem in polar coordinates with Hamiltonian

$$
H = \frac{p_r^2}{2} + \frac{l^2}{2r^2} - \frac{1}{r}.
$$

Introducing the coordinate transformation $r = R^2$, yields the transformed Hamiltonian

$$
H = \frac{p_R^2}{8R^2} + \frac{l^2}{2R^4} - \frac{1}{R^2}.
$$

After a so-called Poincaré time-transformation $g = R^2$, we obtain

$$
\tilde{H} = \frac{p_R^2}{8} + \frac{l^2}{2R^2} - 1 - H_0 R^2. \tag{1}
$$

The singularity at $R = 0$ is of a milder, purely repulsive type. If we attempt to integrate these equations using leapfrog, we would get better resolution through the collision than without regularization, and this improvement is magnified proportionately for higher eccentricity orbits. However, note that whereas leapfrog on the unmodified Kepler problem would reduce to the exact solution away from the collision (where the trajectory reduces to straight line motion), the transformed equations will be unstable far from the collision! The problem is that the use of the time-transformation as part of the regularization process really means that the actual time stepsizes increase without bound along escaping orbits. This problem can be remedied using an outer *Sundman time transformation* which effectively unravels the Poincaré transformation away from the collision point (see Sec. 3.3, below).

For the three-dimensional Kepler problem, we will consider the canonical formulation of the Kustaanheimo-Stiefel spinor transformation [16]. That is, we introduce the mapping in $\mathbf{R^4}$ defined by

$$\begin{bmatrix} q \\ 0 \end{bmatrix} = \phi(Q) = L(Q)Q, \tag{2}$$

where Q is a 4-vector and $L(Q)$ is the KS-matrix

$$L(Q) = \begin{bmatrix} Q_1 & -Q_2 & -Q_3 & Q_4 \\ Q_2 & Q_1 & -Q_4 & -Q_3 \\ Q_3 & Q_4 & Q_1 & Q_2 \\ Q_4 & -Q_3 & Q_2 & -Q_1 \end{bmatrix},$$

with $\frac{1}{|Q|}L(Q)$ an orthogonal matrix. The transformation has the property $|q| = |Q|^2$.

Since

$$\phi'(Q) = 2L(Q),$$

the canonical momenta P corresponding to Q are given by:

$$\phi'^T \begin{bmatrix} p \\ 0 \end{bmatrix} = P \Rightarrow \begin{bmatrix} p \\ 0 \end{bmatrix} = \frac{1}{2|Q|} RP. \tag{3}$$

The KS transformation introduces an S^1 symmetry through the quadratic constraint:

$$Q_4P_1 - Q_3P_2 + Q_2P_3 - Q_1P_4 = 0. \tag{4}$$

To put this another way, ϕ can be viewed as a map from the quotient space $\mathbf{R}^4/S^1$ into $\mathbf{R}^3$. With this interpretation, the inverse map is well-defined and easily computable [16].

In the new variables, the Hamiltonian becomes

$$H = \frac{1}{8}\frac{|P|^2}{|Q|^2} - \frac{1}{|Q|^2}.$$

and after a Poincaré-type time transformation, we get a linear Hamiltonian system:

$$\tilde{H} = |Q|^2(H - H_0) = \frac{1}{8}|P|^2 - 1 - H_0|Q|^2.$$

Assuming that the initial data satisfies (4), this constraint is preserved for all time (i.e. it becomes a first integral).

The Poincaré transformation introduces a nonlinear scaling of time

$$\frac{dt}{ds} = |Q|^2.$$

Resolving the motion thus requires propagation of Q, P as the flow of a simple linear system, coupled to the scalar differential equation

$$\frac{ds}{dt} = |Q(s)|^{-2}.$$

If the solution is needed at a fixed time T, the resolution of the corresponding fictive time $S(T)$ requires the inversion of the antiderivative function for $|Q|^2$. To perform this calculation, we may write

$$F(S) := T - \int_0^S |Q(s)|^2 ds, \tag{5}$$

and use a scalar Newton iteration:

$$S^{(m+1)} = S^{(m)} - \frac{F(S^{(m)})}{F'(S^{(m)})}.$$
$$= S^{(m)} + \frac{F(S^{(m)})}{|Q(S^{(m)})|^2}.$$

Since Q is determined by solving linear differential equations, the formulas can be greatly simplified; but this calculation introduces some overhead in the form of transcendental functions which must be reevaluated several times until convergence.

The method of [18] relies on very frequent computations of two-body problems, including resolution of the inverse time transformation, a somewhat costly process. Good success is reported in [18] using an alternative approach based on the implicit midpoint discretization to solve the KS-transformed equations together with the equation of time. This method is substantially cheaper than using the exact quadrature. The equations reduce to a 4th degree polynomial equation for Δs (see [18] for details) and no transcendental functions need to be evaluated. Although this quartic equation can be solved in radicals, it is much more economical to use a Newton iteration to resolve the time variable.

A standard stopping criterion can be used for the Newton iteration, combining both relative and absolute tolerances. Occasionally, we encountered difficulty with Newton convergence during very close approaches which indicates the use of a more robust modified Newton iteration (see, e.g. [5]). In typical runs, the fast Kepler solver reduced the overall CPU time for the code by a factor of more than 1.5.

Note that the implicit midpoint method is symplectic and preserves all quadratic first integrals, such as the energy in transformed variables and the special constraint (4). For very close approaches, a practical code should probably switch from the approximate fast Kepler solver to the exact Kepler solution.

3.3 Outer Sundman Transformation

The reversible adaptive method of [18] employs a splitting of the Hamiltonian into a Kepler part plus a perturbation. Each of these terms can then be integrated in turn, with the Kepler part handled using the above-described fast Kepler solver.

In addition to the described coordinate and Poincaré transformations, it was found necessary to incorporate an additional outer Sundman transformation in order to obtain good results. The most important use for this additional level of adaptivity is to control the timestep during the unstable close approaches to the nucleus. Here the Kepler problem becomes increasingly sensitive to

perturbations, leading to a numerical instability in the timestepping process and requiring a timestep proportional to $|q|^{-3/2}$ (see [18]).

Another important use of the outer Sundman transformation is to handle variations in force magnitude due to occasional strong perturbation forces, for example due to repulsive electron-electron interactions in an atomic problem. Unlike the extremely wide variations in force observed for the attractive forces, the repulsive forces are usually easily handled with an adaptive timestep.

A third use for the outer Sundman transformation is to limit stepsize growth when the attractive Keplerian force diminishes greatly, e.g. along an escaping trajectory, since the KS transformation would increase the effective timestep arbitrarily.

The rationale for using a Sundman transformation as opposed to an outer Poincaré transformation is strictly practical: if a Poincaré transformation is used, the resulting combined algorithm would include another level of implicitness which would increase the timestep cost several times, whereas the Sundman transformation can be treated using a minor extension of the explicit Adaptive Verlet framework.

3.4 Algorithm: Reversible Adaptive Regularization

The method resulting from combining the techniques of this section is termed the reversible adaptive regularization or RAR method. For convenience, we give a pseudocode algorithm for the RAR methods for treating perturbed Kepler problems and atomic dynamics.

Define:

Kustaanheimo-Stiefel transformation.

$$(Q, P) = \mathrm{KS}(q, p),$$

obtained by solving (2), (3) (with arbitrary choice of the gauge freedom) for Q, P, (see [16] for formulae) and corresponding inverse map:

$$(q, p) = \mathrm{KS}^{-1}(Q, P),$$

defined directly by equation (2),(3).

KS Time Transformation.

Compute $\Delta s = \mu(\Delta t)$ by solving the midpoint approximation to the time relation (5) using a Newton iteration. (During very close approaches, we instead do not introduce the midpoint approximation.)

KS Solve.

Compute $(\hat{Q}, \hat{P}) = \Phi_{\Delta s}(Q, P)$, the solution of the linear system (1) in the transformed variables using implicit midpoint with timestep Δs. This requires the solution of 2×2 linear systems. (During very close approaches, instead solve (1) for a time interval Δs.)

Outer Sundman Transformation.

Define control function g by

$$g(q) = (1 + |q|^{-a})^{-1},$$

where a is a fixed positive parameter.

Perturbed Kepler Problem Timestep Algorithm

Given: $\Delta\tau$ fixed, q^0, p^0, initial (previous) timestep Δt_0, this algorithm applies the RAR method to solve

$$H = \frac{1}{2}|p|^2 - \frac{1}{|q|} + \hat{H}(p, q).$$

for one fictive timestep $\Delta\tau$, yielding (q^1, p^1).

1. Compute the new timestep by

$$\Delta t_1 := \left(\frac{2}{g(q^0)} - \frac{\Delta\tau}{\Delta t_0} \right)^{-1} \Delta\tau.$$

2. Solve the perturbation Hamiltonian $\hat{H}$ for a timestep of size $\frac{1}{2}\Delta t_1$, using either the exact solution (if easily computed) or an approximation. Store result in $(\hat{q}_0, \hat{p}_0)$.

3. $(Q^0, P^0) := \mathrm{KS}(\hat{q}^0, \hat{p}^0)$.

4. Compute KS timestep $\Delta s := \mu(Q^0, P^0, \Delta t_1)$.

5. Compute KS solution $(Q^1, P^1) := \Phi_{\Delta s}(Q^0, P^0)$.

6. $(\hat{q}^1, \hat{p}^1) := \mathrm{KS}^{-1}(Q^1, P^1)$.

7. Repeat step (2) from $(\hat{q}^1, \hat{p}^1)$. Result is (q^1, p^1).

Note: The fictive timestep computation (step 4.) can be accelerated by use

of a good predictor for the new Δs. We had good results by storing Δs_n at the nth timestep and then using as predictor

$$\Delta s^{\mathrm{P}}_{n+1} := \frac{\Delta t_{n+1}}{\Delta t_n} \Delta s_n,$$

in the Newton iteration defining μ.

3.5 Adjustments for Mono-Atomic Systems

For the mono-atomic problem, the same procedure is applied for each of the electrons in the system. The only modifications to the algorithm are as follows.

(i) We replace the time transformation by

$$g(q) = (1 + r_{\mathrm{en}}^{-a} + r_{\mathrm{ee}}^{-b})^{-1},$$

where $r_{\mathrm{en}} = \min_i |q_i|$, and $r_{\mathrm{ee}} = \min_{i \neq j} |q_i - q_j|$.

(ii) The perturbation Hamiltonian at steps 2. and 7. is replaced by the electron-electron interaction potential.

(iii) The fast KS solve in steps 3.-6. is performed for each of the N electrons in the system.

(iv) Fictive timestep values should be stored for each electron, in order to predict Δs for each electron to improve convergence of the timestep iteration (step 4.).

4 Applied Fields

In this section, we show how applied electrical and magnetic fields can be incorporated into the reversible adaptive regularization method, an important aspect since Rydberg atom systems typically involve such fields [4,19]. Through splitting, we first reduce a multiple electron atom to individual electron-nucleus interactions, i.e. the hydrogenic case. For hydrogen, the Hamiltonian in constant electrical and magnetic fields is

$$H = \frac{1}{2}|p - \frac{1}{2}\hat{B}q|^2 - \frac{1}{|q|} + E \cdot q,$$

with $E \in \mathbf{R}^3$, $B = (b_1, b_2, b_3)^T \in \mathbf{R}^3$ and

$$\hat{B} = \text{skew}(B) = \begin{bmatrix} 0 & b_3 & -b_2 \\ -b_3 & 0 & b_1 \\ b_2 & -b_1 & 0 \end{bmatrix}.$$

For the case of parallel static magnetic and electrical fields, it is convenient to represent the problem in semi-parabolic coordinates, as in [28]. To do this, assume that $E = (0, 0, \sigma)$ and $B = (0, 0, \gamma)$ are fixed. The key observation is that the z-component of angular momentum remains an invariant (the Hamiltonian possesses rotational symmetry about the z-axis). We introduce polar coordinates,

$$H = \frac{1}{2}(p_r^2 + p_z^2) + \frac{l^2}{r^2} + \frac{\gamma l}{r} + \frac{1}{8}\gamma^2 r^2 - \frac{1}{r^2 + z^2} + \sigma z,$$

where l is the angular momentum, and follow this with the change of variables $r = u^2 - v^2$, $z = 2uv$. After a time transformation $g = u^2 + v^2$, we find

$$\begin{aligned}\tilde{H} = \frac{1}{8}(p_u^2 + p_v^2) + \frac{l^2(u^2 + v^2)}{(u^2 - v^2)^2} + \frac{\gamma l}{u^2 - v^2} + \frac{1}{8}\gamma^2(u^2 - v^2)^2(u^2 + v^2) - 1 \\ +2\sigma uv(u^2 + v^2) - H_0(u^2 + v^2).\end{aligned}$$

This approach, when combined with a reversible-adaptive integrator such as Adaptive Verlet can lead to rather good behavior [28], especially when $l = 0$ and the singular terms vanish. For arbitrary field alignments, or for moving fields, the angular momentum is no longer a conserved quantity, and a more general approach is needed.

4.1 A splitting method for fields

For the general case we propose to introduce the splitting $H = H^{\text{Kep}} + H^{\text{B}} + H^{\text{E}}$, with

$$H^{\text{Kep}} = \frac{|p|^2}{2} - \frac{1}{|q|}, \qquad H^{\text{B}} = -\frac{1}{2}(p^T \hat{B} q - \frac{1}{8} q^T \hat{B}^2 q), \qquad H^{\text{E}} = E \cdot q.$$

The first part can be integrated using the KS-transformation (or the fast Kepler solver). In the case of constant fields, the second and third parts are

integrable: under H^{B}, q can be evolved from q^{old} to q^{new} via a rotation about B,

$$q^{\mathrm{new}} = \exp(-\frac{1}{2}\Delta t \hat{B}) q^{\mathrm{old}},$$

which is easily and efficiently computed using Rodrigue's formula:

$$\exp(\alpha \hat{B}) = \cos(\alpha|B|)I + \frac{\sin(\alpha|B|)}{|B|}\hat{B} + \frac{(1-\cos(\alpha|B|)}{|B|^2}BB^T.$$

Then the corresponding update to p can be obtained by solving the resulting 3×3 linear system

$$\dot{p} = -\frac{1}{2}\hat{B}p - \frac{1}{4}\hat{B}^2 q.$$

In a timestep, this yields

$$\begin{aligned} p^{\mathrm{new}} &= \exp(-\frac{1}{2}\Delta t \hat{B}) p^{\mathrm{old}} - \frac{1}{4}\int_0^{\Delta t} \exp(-\frac{1}{2}(\Delta t - \tau)\hat{B})\hat{B}^2 \exp(-\frac{1}{2}\tau \hat{B}) q^{\mathrm{old}} ds, \\ &= \exp(-\frac{1}{2}\Delta t \hat{B})(p^{\mathrm{old}} - \frac{1}{4}\Delta t \hat{B}^2 q^{\mathrm{old}}), \end{aligned}$$

where we have used the fact that the exponential of $\hat{B}$ commutes with $\hat{B}$. Thus just a single additional rotation about B is needed. Finally, the electrical field term is p-independent and therefore also easily integrated.

We use a symmetric splitting, the Sundman transformation of the last section, and the Adaptive Verlet method to combine the various parts into a usable method. The justification for using such a splitting is that during the critical close approaches to the nucleus, we have,

$$\begin{aligned} |p| &\sim |p - \frac{1}{2}\hat{B}q|, \\ &\sim \sqrt{2\left(H_0 + \frac{1}{|q|}\right)}, \\ &\sim \sqrt{2}|q|^{-1/2}, \end{aligned}$$

where we have used the conservation of energy. Thus the force contribution from the magnetic field term is on the order of the fourth root of the Coulombic force in this regime. Other perturbations are typically even smaller.

In the absence of ionizing trajectories, the presence of fields does not require any modification of the time transformation. [2]

4.2 Time-Dependent Fields

Various types of microwave and laser fields can be described by introducing time-dependencies in the electrical and magnetic fields. For example, a typical sinusoidal laser field is described by a term of the form

$$H_{\mathrm{L}} = \mu(r) F \sin(\omega t + \varphi),$$

where ω is the frequency, F the amplitude, and φ is a phase shift. μ is the direction of the field. Integrating such a term is completely straightforward.

A time-dependent magnetic field is not necessarily exactly integrable, in which case this portion of the update can be performed using the implicit midpoint method at relatively low expense.

4.3 Numerical experiment: hydrogen in parallel fields

We apply this method to treat hydrogen in parallel fields. As noted at the beginning of the section, this problem can be solved using semiparabolic coordinates; it is interesting that the general reversible adaptive regularization method, which does not specifically make use of the known angular momentum, also performs well.

We fixed $E = (0, 0, 1)$, set $B = (0, 0, \gamma)$, and varied γ, plotting electron positions for $t \in [0, 500]$ using fictive stepsize $\Delta s = 0.01$. For small values of γ, the electron motion appears to be quasiperiodic (Fig. 1, top, $\gamma = 0.6$). For larger values, the orbit becomes ergodic and fills a region of space (Fig. 1, center, $\gamma = 4$). (The darkening in the center is not a reflection of the physical density of trajectories there; it is an artifact of the larger numbers of timesteps placed near the origin due to the step control.) Near $\gamma = 6$ a two-dimensional

[2] For ionizing orbits in electrical and magnetic fields, some adjustment of the time transformation is necessary in order to accurately follow escaping trajectories. We obtained good results by simply modifying the step control function g to

$$g(q) = \frac{1}{r_{\mathrm{en}}^{-a} + r_{\mathrm{ee}}^{-b} + r_{\mathrm{max}} + 1},$$

where r_{max} represents the largest radial component of any of the electron components.

structure begins to emerge, and is refined at about $\gamma = 8$ (Fig. 1, bottom). The graphs are suggestive of tori motion, indicating the presence of a nearby periodic orbit. At $\gamma = 7.796$, and $E = (0, 0, 1.012625)$ we indeed find such a periodic orbit (Fig. 2), making approaches within $|q| = 10^{-7}$ of the nucleus. Periodic orbits very similar to this one are mentioned in [9], and are important to the current understanding of the semiclassical theory. Despite the close approaches, the stepsize is smoothly controlled during the collision, and the energy is strikingly well-behaved (Fig. 3). Observe in particular that during close approach, the orbit takes the appearance of a pure Kepler orbit (with the associated symmetry properties).

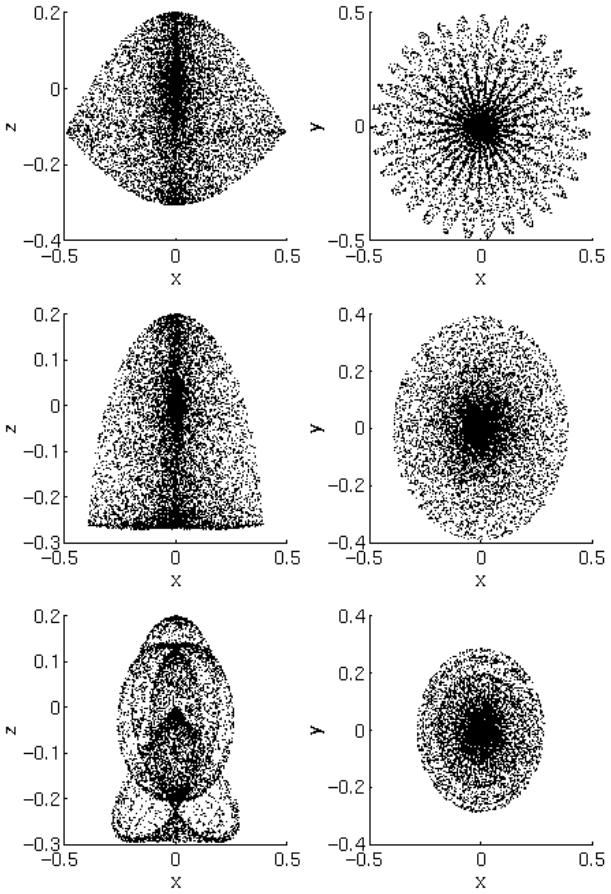

Fig. 1. Side and top views of orbits of hydrogen in parallel fields: top $\gamma = 0.6$, center $\gamma = 4$, and bottom, $\gamma = 8$.

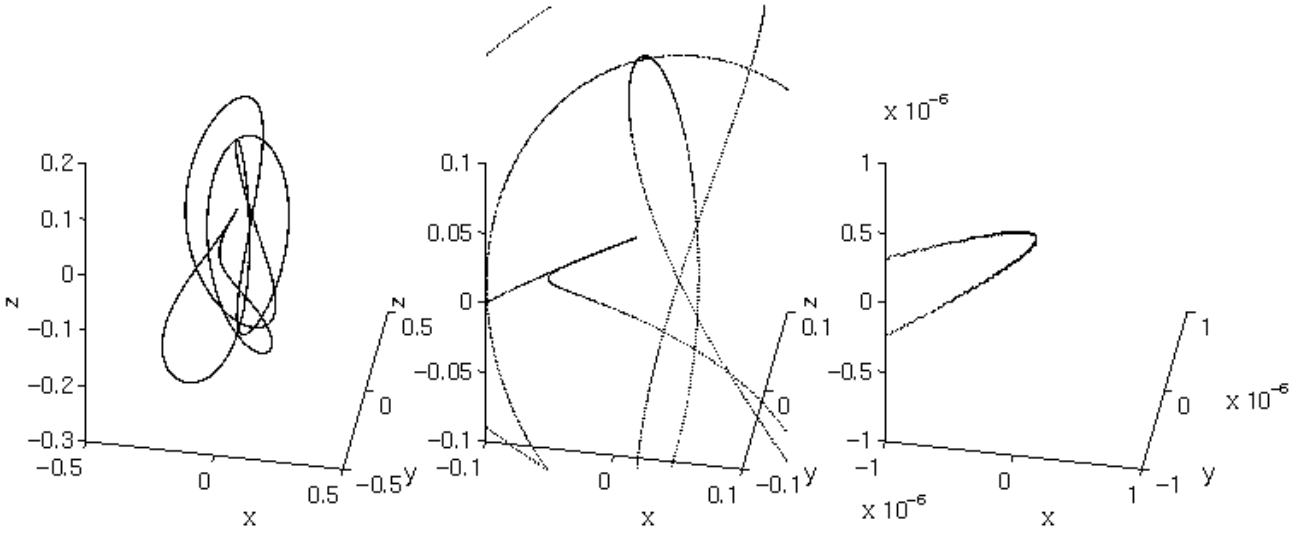

Fig. 2. Periodic orbit at At $\gamma = 7.796$, and $E = (0, 0, 1.012625)$, with close-ups of the origin.

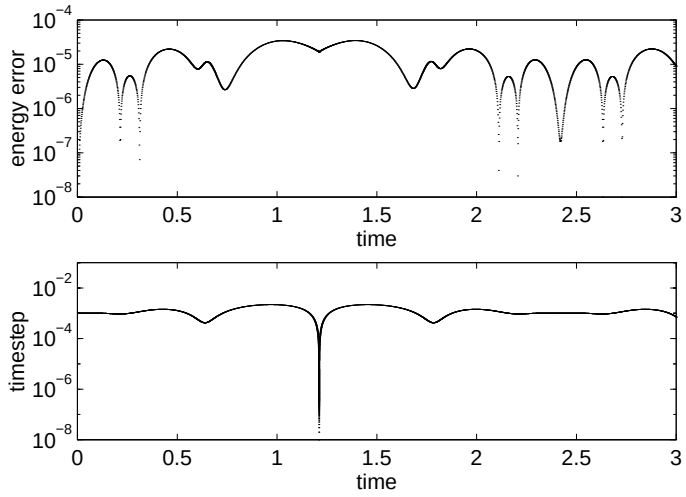

Fig. 3. Energy variation and timestep variation over approximately one period of the motion. Despite the requirement for small steps in the vicinity of the origin, the energy is very well controlled. Longer simulations revealed no noticeable drift in energy.

References

[1] Aarseth, S.J., Direct methods for N-body simulation, in *Multiple Time Scales*, eds. J.U. Brackbill and B.I. Cohen, Academic Press, NY, 1985.

[2] E. Barth, B. Leimkuhler and S. Reich, A semi-explicit, variable stepsize, time-reversible integrator for constrained dynamics, preprint, 1996.

[3] G. Benettin and A. Giorgilli, On the Hamiltonian interpolation of near-to-the-identity symplectic mappings with application to symplectic integration algorithms, J. Statist. Phys. **74**, 1117, 1994.

[4] F. Benvenuto, G. Casati, and D. Shepelyansky, Dynamical localization: hydrogen atoms in magnetic and electrical fields, Phys. Rev. **A 55**, 1732, 1997.

[5] R. Bulirsch and J. Stoer, *Introduction to Numerical Analysis*, Springer, 1980.

[6] G. Ezra, K. Richter, G. Tanner, and D. Wintgen, J. Phys. **B 24**, L413, 1991

[7] J. Frank, W. Huang and B. Leimkuhler, Geometric Integrators for Classical Spin Systems, J. Comput. Phys., to appear, 1997.

[8] Y. Funato, P. Hut, S. McMillan, and J. Makino, Time-Symmetrization of Kustaanheimo-Stiefel Regularization, Astrophysics J. **112**, 1697, 1996.

[9] M. Gutzwiller, *Chaos in Classical and Quantum Mechanics*, Springer, NY, 1990.

[10] E. Hairer, Variable timestep integration with symplectic methods, preprint, Dept. of Mathematics, Geneva, 1996.

[11] D.C. Heggie, Cel. Mech. **10**, 185, 1974.

[12] D.C. Heggie, The N-body problem in stellar dynamics, in *Long-Term Dynamical Behavior of Natural and Artificial N-Body Systems*, Ed. A.E. Roy, Kluwer, Dordrecht, 1988.

[13] W. Huang and B. Leimkuhler, The Adaptive Verlet Method, SIAM J. Sci. Comp. **18**, 239, 1997.

[14] P. Hut, J. Makino, S. McMillan, Building a better leapfrog, The Astrophysical Journal **443**: L93-L96, 1995.

[15] P. Hut, Funato, Y., Kokubo, E., J. Makino, S. McMillan, Time symmetrization meta-algorithms, in *Computational Astrophysics,* Proc. of the 12th 'Kingston meeting' on Theoretical Astrophysics, Eds. D.A. Clarke and M.J. West, ASP Conf. Series, to appear.

[16] P. Kustaanheimo and E. Stiefel, Perturbation theory of Kepler motion based on spinor regularization, J. Reine Angew. Math., **218**, 204, 1965.

[17] E. Lee, A. Brunello, and D. Farrelly, Coherent states in a Rydberg atom: classical mechanics, Phys. Rev. **A 55**, 2203, 1997.

[18] B. Leimkuhler, Reversible Adaptive Regularization: Perturbed Kepler Motion and Classical Atomic Trajectories, preprint (Numerical Analysis Reports, DAMTP, Cambridge, 1997), submitted to Phil. Trans. Roy. Soc.

[19] J. Main and G. Wunner, Hydrogen atom in a magnetic field: ghost orbits, catastrophes, and uniform semiclassical approximation, J. Phys. **A 55**, 1743, 1997.

[20] S. Reich, Backward error analysis for numerical integrators, preprint, 1996.

[21] K. Richter, and Wintgen, W., J. Phys. **B 23**, L197 1990.

[22] K. Richter, G. Tanner, and W. Wintgen, J. Phys. **A 48**, 4182 1993.

[23] R.D. Ruth, A canonical integration technique, IEEE Trans. Nucl. Sci. **30**, 2669, 1983.

[24] K. Rzazewski, M. Lewenstein, and P. Salieres, Multielectron stabilization of atoms in a laser field: classical perspective, Phys. Rev. **A 49**, 1196, 1994.

[25] J.M. Sanz-Serna and M.P. Calvo, *Numerical Hamiltonian Problems*, Chapman and Hall, 1994.

[26] C.L. Siegel, and J.K. Moser, *Lectures on Celestial Mechanics*, Springer, Berlin, 1971.

[27] D. Stoffer, Variable steps for reversible integration methods, Computing **55**,1, 1995.

[28] Q. Wang and A. Starace, Classical interpretation of the quantum description of H^- photodetachment in parallel E and B fields, Phys. Rev. A **55**, 815, 1997.